Applied Physics A (2021) 127:962
https://doi.org/10.1007/s00339-021-05069-5

Applied Physics A
Materials Science & Processing

PbF_2–TeO_2 glasses and glass–ceramics: a study of physical and optical properties

E. F. El Agammy[1,2] · H. Doweidar[2] · K. El-Egili[2] · R. Ramadan[3]

Received: 31 August 2021 / Accepted: 3 November 2021 / Published online: 28 November 2021

Abstract
Some physical and optical properties of $x$$PbF_2$·(100–$x$)$TeO_2$ ($0 \le x \le 90$ mol%) glasses and glass–ceramics have been studied. Density increases linearly with increasing PbF_2 content up to 70 mol% PbO, then tends to be constant for $70 < PbF_2 \le 90$ mol%. The molar volume remains constant in the first region then increases for $PbF_2 > 70$ mol%. The main factor which controls the molar volume is the change in free volume and packing density. There is a limited increase in conductivity with increasing PbF_2 content then it decreases for $PbF_2 \ge 50$ mol%. Pb^{2+} ions are the main charge carriers. The band gap E_g and the linear refractive index n change in an opposite manner where E_g increases with increasing PbF_2 content for $PbF_2 \le 50$ mol%, then it decreases sharply for $PbF_2 > 70$ mol%. For $PbF_2 \le 50$ mol%, the Urbach energy E_U decreases then seems to be constant for further additions. Metallization criterion M and molar refractivity R_m change in a similar manner to E_g and n, respectively.

Keywords PbF_2 · TeO_2 glasses and glass–ceramics · Density · Energy gap · Conductivity

1 Introduction

Glasses containing oxide-fluoride systems have good optical properties and perfect thermal and chemical stability [1]. PbF_2 was able to form stable glasses due to its dual role as a modifier and former [2]. PbF_2 glasses can be believed as appropriate candidates for electrochemical applications [3], like power sources, particularly in the scope of solid-state batteries. Besides, they have prospective applications in IR fiber optics and laser windows [4].

The density of $x$$PbO_2$·(100-$x$)$TeO_2$ ($13.6 \le x \le 21.8$ mol%) and $x$$PbF_2$·(100-$x$)$TeO_2$ ($13.7 \le x \le 26$ mol%) glasses was measured [5]. It is found that it increases with increasing PbO and PbF_2 content, respectively. Also, the electrical conductivity of $x$$PbF_2$·(100-$x$)(PbO:$TeO_2$) ($0 \le x \le 60$ mol%) glasses was studied by El Damrawi [6], it is stated that replacing PbO and TeO_2 by PbF_2 decreases the activation energy for conduction and increases the conductivity. The increase in conductivity is due to the increase in both the concentration and mobility of charge carriers. Transport of fluorine ions in those glasses is explained by the random site model.

The UV spectra of TeO_2-PbF_2 glasses were measured by Shiqing et al. [7]. It is found that with adding PbF_2 into tellurite glasses, the excitation energy of the absorption band decreases. This is because the polarizability of O^{2-} is higher than that of F^-. In addition, F^- ions can break oxygens of the network (making them NBOs) and tighten the mobility gap.

In this work, we aim to study the density, electrical conductivity and optical properties of $x$$PbF_2$·(100–$x$)$TeO_2$ glasses and glass–ceramics. Also, explore the role of F^- and Pb^{2+} ions in conductivity. This is an extended work of a previous study on the structure of these glasses [8].

2 Experimental

As start materials with high purity (99%, Sigma-Aldrich), reagent grades of PbF_2 and TeO_2 were used to prepare the investigated glasses and glass–ceramics. Batches were

✉ E. F. El Agammy
e.f.elagamy@gmail.com

✉ H. Doweidar
hdoweidar@mans.edu.eg

[1] Physics Department, College of Science, Jouf University, P.O. Box: 2014, Sakaka, Saudi Arabia

[2] Glass Research Group, Physics Department, Faculty of Science, Mansoura University, Mansoura 35516, Egypt

[3] Microwave Physics and Dielectrics Department, Physics Research Institute, National Research Centre, Dokki, Cairo 12311, Egypt

melted in silica crucibles for 25 min, at 780–830 °C, depending on their respective compositions. The crucible was swirled repeatedly until the melt became visually homogeneous. Glass disks were obtained at room temperature after the melt was dropped on a steel plate and compressed by another one.

The density (D) was determined by applying the standard Archimedes method at room temperature for four samples of each glass. The used immersion liquid was Xylene. Density values are accurate to ± 2%.

The dc conductivity was determined by measuring the resistance in the range of 10^3–10^{13} Ω for samples with a thickness ranging between 1.5–3 mm. About ± 0.04 eV and ± 5% are considered as experimental errors for the activation energy and conductivity, respectively.

To determine the optical transition the optical properties were measured by UV–Visible–NIR Spectrophotometer (JASCO model V770) in the range 190–2000 nm through absorption spectra.

3 Results and discussion

3.1 Density and molar volume

Figure 1 shows the change of density D and the molar volume (V_m) with PbF_2 content. It is clear that D increases linearly with increasing PbF_2 content up to 70 mol% then it seems to have steady values with further additions of PbF_2. The increase in D with increasing PbF_2 content may be due to that the molecular mass of PbF_2 (245.1968 g/mol) is larger than that of TeO_2 (159.5988 g/mol). Nevertheless, the constancy of D for $PbF_2 \geq 70$ mol% indicates that the latter assumption is not the sole reason for increasing density. In $xPbF_2 \cdot (1-x)B_2O_3$ glasses where ($30 \leq x \leq 80$), Doweidar et al. [9] mentioned that

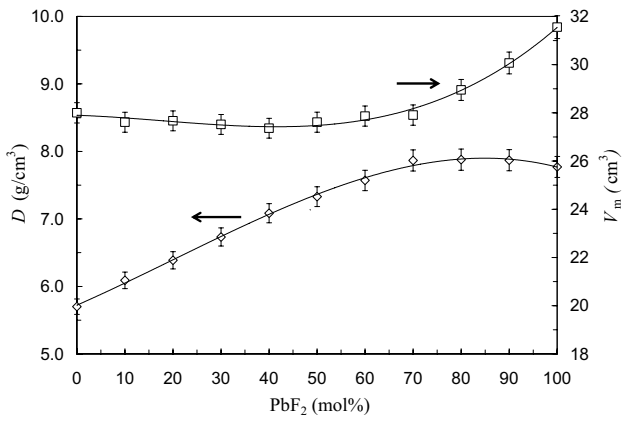

Fig. 1 Experimental density and molar volume as a function of PbF_2 content. Density and molar volume values are accurate to ± 2 and ± 1.5%, respectively

the density of the glasses increases with increasing PbF_2 content. Also, the overall density of the structural units formed with addition of PbF_2 in the matrix ($Pb^{2+}_{1/2}[TeO_{3+1}]^-$, $TeO_{3/2}F$ and PbF_2) [8] is larger than that of TeO_4 ones and this leads to an increase in density. Vogel et al. [5] mentioned that in PbF_2–TeO_2 glasses, density increases with increasing PbF_2 content.

Figure 1 represents the dependence of molar volume (V_m) on PbF_2 content. The V_m can be estimated from the experimental density data and the molecular mass (M) of glass by the following relation.

$$V_m = M/D. \tag{1}$$

There is no change in V_m for compositions with $PbF_2 \leq 70$ mol%, then it increases for $PbF_2 > 70$ mol%. The constancy of V_m for $PbF_2 \leq 70$ mol% points out to the dependence of D on the molecular mass. The change of V_m with PbF_2 content (Fig. 1) might be correlated with the change in packing density (P_d) and free volume (V_f). The free volume (V_f) can be given as

$$V_f = V_m - \sum m_i V_i \tag{2}$$

where m_i is the number of ions (i) and V_i is the volume of such ion of type (i) whereas the later can be expressed as

$$V_i = (4/3)\pi r_i^3 \tag{3}$$

r_i denotes the radius of ion of type (i) [10] and i refers to Te^{4+}, O^{2-}, Pb^{2+} and F^- ions. V_i includes the volume of atoms and/or ions inside the unit and its surrounding space in the glass matrix. The packing density of the oxides can be given as [11]

$$P_d = \sum m_i V_i / V_m \tag{4}$$

Figure 2 shows the change of free volume and packing density with PbF_2 content. It is obvious from Fig. 2 that V_f has almost constant values for $PbF_2 \leq 50$ mol% and increases gradually for $PbF_2 > 50$. However, P_d behaves in a different manner at higher concentrations where it decreases gradually for $PbF_2 > 50$ mol%, while constant for $PbF_2 \leq 50$ mol%. The constancy of V_f and P_d in the composition range $0 \leq PbF_2 \leq 50$ might be the reason for the constancy in V_m. In addition, the volumes of the structural units related to PbF_2 and those for TeO_2 have convergent values. Also, for $PbF_2 > 50$ mol% the increase in V_f and the decrease in P_d may be responsible for the increase in V_m of the glass and the constancy of density D for $PbF_2 > 70$ mol%.

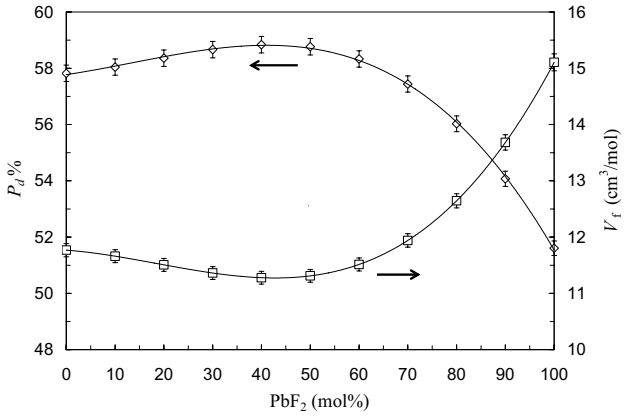

Fig. 2 Dependence of the free volume (V_f) and packing density (P_d) on the PbF_2 content. V_f and P_d values are accurate to ± 1 and ± 0.5%, respectively

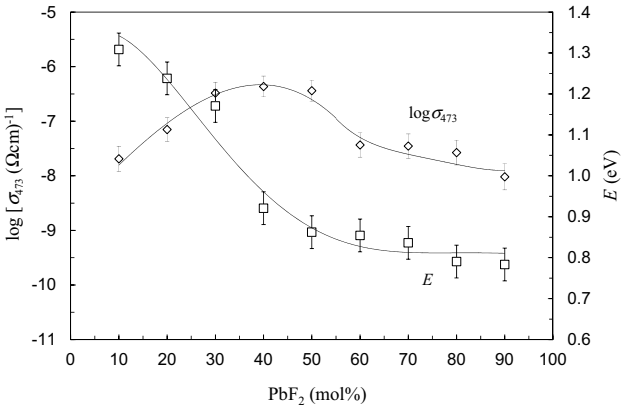

Fig. 4 The electric conductivity's natural logarithm at 473 K and the activation energy as a function of PbF_2 content

3.2 Electric conduction

Figure 3 shows the variation of the natural logarithm of the direct current electrical conductivity (logσ) with the reciprocal of absolute temperature (1000/T) in PbF_2–TeO_2 glasses and glass–ceramics. The change of logσ with 1000/T is linear which reveals that the conduction process is ionic in nature according to Arrhenius equation

$$\sigma = \sigma_o \exp(-E/kT). \quad (5)$$

Here σ_o is a constant. T, k and E are absolute temperature, activation energy for the conduction process and Boltzmann's constant, respectively.

Figure 4 shows the change of logσ_{473}log conductivity at 473 K) and E with PbF_2 content. There are two regions

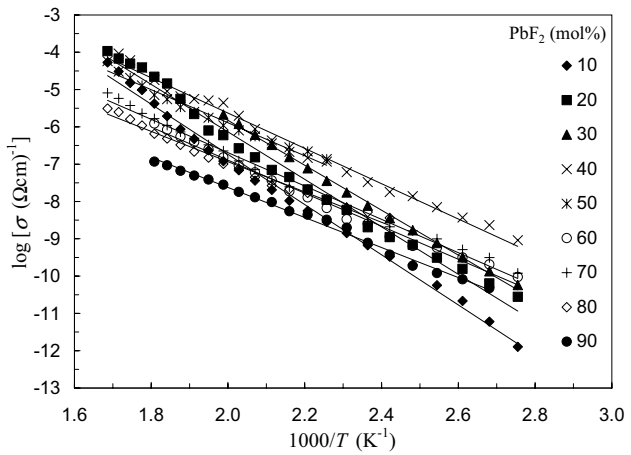

Fig. 3 Electric conductivity–temperature dependence of PbF_2–TeO_2 glasses and glass–ceramics

in the change of log$\sigma_{473}$and E. The first region is for $PbF_2 \leq 50$ mol% where the conductivity increases by about 1.3 orders with increasing PbF_2 content. However, in this region E decreases linearly with increasing PbF_2 content. The second region is for $PbF_2 \geq 50$ wherewith increasing PbF_2 content logσ_{473} decreases steadily up to 90 mol% PbF_2. In this region, E seems to be nearly constant.

The conductivity [12] is given by the following relation

$$s = cq\mu \quad (6)$$

where q, c and μ are, respectively, the ionic charge, the concentration of mobile ions and the mobility of charge carrier. It is understood from Eq. (6) that σ depends on c and/or μ. El Agammy et al. [8] showed that in the studied glasses N_4 (the fraction of four coordinated tellurium atoms) decreases for $PbF_2 \leq 30$ mol% and the majority of F^- ions enters the glass structure as terminal ones to convert TeO_4 units to $(Pb^{2+}_{1/2}[TeO_{3+1}]^-$ and $TeO_{3/2}F)$ units. A similar behavior of N_4 was shown in NaF–TeO_2 glasses and glass–ceramics [13]. As the increase in conductivity for $PbF_2 \leq 50$ mol% is only 1.3 orders of magnitude and the electronegativity of F atom (3.98) is greater than that of O atom (3.44), we can infer that the bonding energy of Te–O is smaller than that of Te–F [14], it is presumed that the main charge carriers are Pb^{2+} ions and the transport of these ions is responsible for the conduction process. Considering that the conductivity depends on c and/or μ, where the mobility represents the possibility of ease in movement of the ions under an external electric field. When PbF_2 was modified up to 50 mol%, σ increased by just 1.3 orders. This might be due to the ionic radius of Pb^{2+} ions (1.19 Å) and the dependence of the free volume on PbF_2 content.

As shown in Fig. 2, V_f is nearly constant up to 50 mol% PbF_2. In this region, the number of charge carriers increases (Pb^{2+} ions) by adding PbF_2. It is then assumed

that the constancy in V_f might limit the increase in the conductivity. Doweidar et al. [15] found a confined increase in conductivity in $x CaF_2 \cdot (100–x) B_2O_3$ glasses. They stated that a decrease in V_f with increasing CaF_2 content leads to a decrease in the mean mobility. Replacing TeO_2 by PbF_2 increases the charge carriers and might decrease the activation energy in this region.

In the second region ($PbF_2 > 50$ mol%), there is a gradual decrease in $\log\sigma_{473}$ (Fig. 4) and E is nearly constant. For $PbF_2 > 50$, it is confirmed by X-ray diffraction and transmission electron microscopy [8] that amorphous and crystalline PbF_2 are the major phases in these glasses and glass–ceramics. Also, SEM [8] shows agglomerates of these phases as clusters of different sizes. Despite the increase of V_f and c for $PbF_2 \geq 50$ mol%, there is a decrease in $\log_{473}$ and E is nearly constant. This may be due to that the majority of PbF_2 that enters the matrix tends to form its own crystalline and amorphous matrix as clusters which are not connected to each other's [8]. Also, the matrix of PbF_2 might be the dominant in the glass in this region. This separation makes the continuous migration of Pb^{2+} in continuous pathways of charge carriers more difficult and limits the conductivity. The bonding energy of Te–F bond is ~ 683.7 eV [14] and that of Pb–F is about 684.1 eV [16], which are close to each other's. This leads to the assumption that F^- ions do not contribute in the conduction process and the association of lead and fluorine ions may hinder the diffusion of the Pb^{2+} ions which might limit the conductivity.

3.3 Optical properties

3.3.1 Optical absorption spectra, optical band gap and refractive index

The optical absorption spectra of $x PbF_2 \cdot (100\text{-}x) TeO_2$ glasses and glass–ceramics ($10 \leq x \leq 90$ mol%) plotted as a function of the wavelength in the range of 190–2000 nm as shown in Fig. 5. The fundamental absorption peak is centered at ~ 280 nm and then with increasing PbF_2 content, especially for $PbF_2 > 70$ mol%, it shifts to higher wavelengths. The optical absorbance A is related to the absorption coefficient α through the equation [17],

$$\alpha(\mathrm{cm})^{-1} = 2.303(A/d) \tag{7}$$

where d is the sample thickness. In Davis and Mott equation [18],

$$(\alpha h\upsilon)^{1/m} = B\left(h\upsilon - E_g\right) \tag{8}$$

where B is a constant, m is an indicator that locates the optical transition type, h, E_g and υ are Planck's constant, optical band gap and photon's frequency. The optical transition type must take the following values $m = 1/2$ and 2 for direct and indirect transition, respectively. Moreover, it is stated by many others [19–23] that indirect allowed transitions ($m = 2$) are valid for oxide glasses.

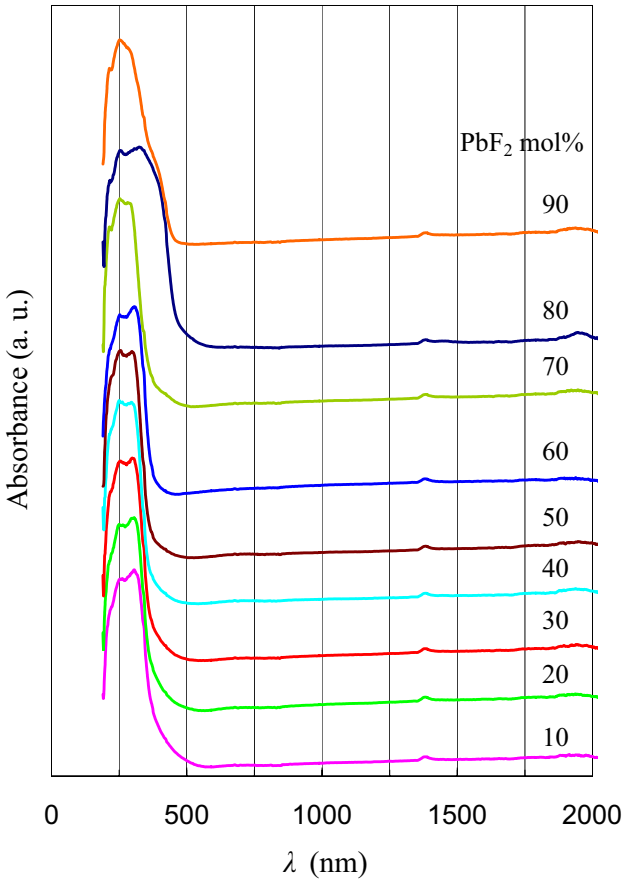

Fig. 5 Absorption spectra of PbF_2–TeO_2 glasses and glass–ceramics

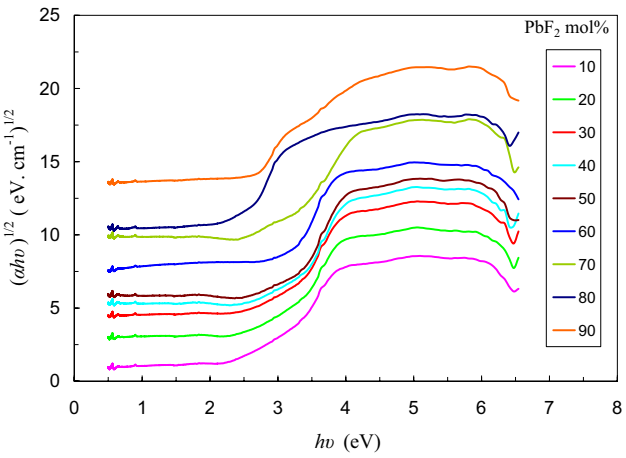

Fig. 6 Plots of $(\alpha h\upsilon)^{1/2}$ versus $h\upsilon$ for PbF_2–TeO_2 glasses and glass–ceramics

Depending on that, Tauc plots were used to estimate the optical band gap. Figure 6 represents Tauc plots for the

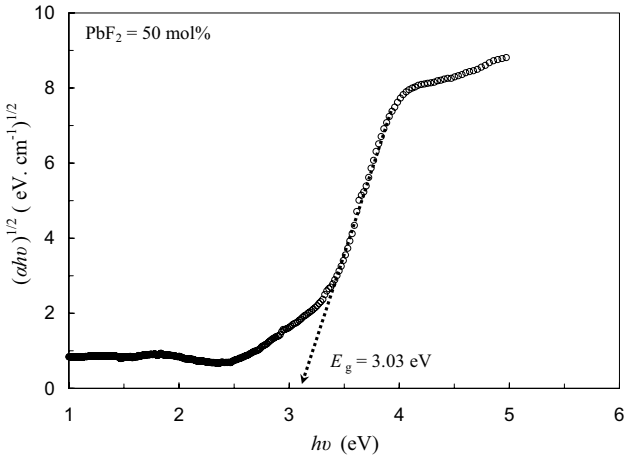

Fig. 7 Determination of the optical band gap E_g for indirect transition for the sample ($PbF_2 = 50$ mol%)

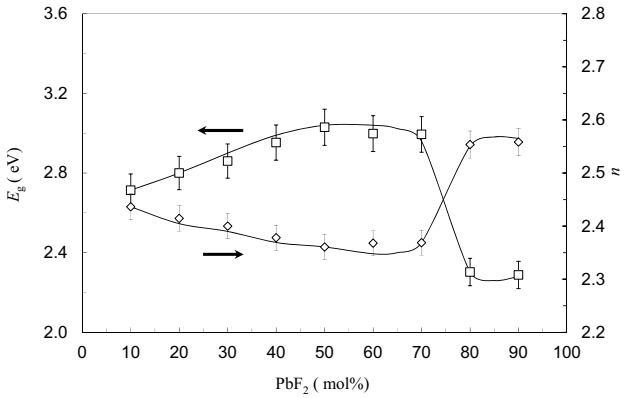

Fig. 8 Dependence of the linear refractive index n and band gap E_g on PbF_2 content

variation of $(\alpha h\nu)^{1/2}$ versus $(h\nu)$. Figure 7 shows the method of estimating E_g [24–26]. Figure 8 shows the variation of the band gap on the content of PbF_2. There are three regions for the variation. The first is for $PbF_2 \leq 50$ mol% where E_g increases with increasing PbF_2 content. The second is for $50 \leq PbF_2 \leq 70$ mol% where E_g is nearly constant. The last is for $PbF_2 > 70$ mol% where E_g decreases sharply then becomes constant. In the first region, E_g value varies from 2.7 to 3.03 eV. Previously, El Agammy et al. [8] deduced that in the studied glasses, PbF_2 completely modifies the structure for $PbF_2 \leq 10$ mol% and plays the dual role (former and modifier) for $PbF_2 > 10$ mol%. In addition, the modifier PbF_2 converts TeO_4 units to $Pb^{2+}_{1/2}\left[TeO_{3+1}\right]^-$ and $TeO_{3/2}F$ units, while former PbF_2 builds its own matrix. The increase of E_g in the first region might be due to that the rate of increase in $C_{Pb(f)}$ (former part of PbF_2 (mol%)) is high [8], in contrary $C_{Pb(m)}$ (modifier part of PbF_2 (mol%)) seems to decrease with low rate through this region. When $C_{Pb(m)}$ increases it is expected that the concentration of NBO bonds increases in the matrix [8]. In this case, the increase in $C_{Pb(f)}$ and decrease in $C_{Pb(m)}$ might decrease the rate of forming NBO, and as a result E_g increases [23, 27, 28]. The constancy and the decrease in the second and last regions might be due to that the PbF_2 matrix becomes the dominant one, rather than the TeO_2 matrix. In addition, the sudden decrease that occurred for $PbF_2 > 70$ mol% might be due to the formation of more ordered structure and the noticed existence of PbF_2 crystalline phases in this region [8]. Also, the main matrix seems to be mainly saturated with PbF_2. In addition, Fig. 2 shows that V_f has almost constant values for $PbF_2 \leq 50$ mol% and increases gradually for further additions of PbF_2. However, P_d behaves in a different manner at higher concentrations. The increase in V_f and decrease in P_d for $PbF_2 > 50$ mol% may be responsible for increasing the molar volume of the glass and decreasing E_g in this range.

Table 1 presents the values of the band gap, linear refractive index, molar volume, molar refractivity, metallization criterion and Urbach energy. Figure 8 shows the variation of the linear refractive index n on PbF_2 content. The refractive index n for glasses has been correlated to the band gap as follows [29],

$$\frac{n^2-1}{n^2+2} = 1 - \sqrt{\frac{E_g}{20}} \tag{9}$$

where the value 20 in this relation has dimension eV according to Duffy [30]. There are three regions for the variation of

Table 1 Optical band gap E_g, linear refractive index n, molar volume V_m, molar refractivity R_m, metallization criterion M and Urbach energy E_U

x (mol%)	E_g (eV)	n	V_m (cm^3)	R_m (cm^3)	M	E_U (eV)
10	2.71	2.48	27.61	17.44	0.368	0.54
20	2.80	2.45	27.67	17.32	0.374	0.47
30	2.86	2.44	27.52	17.11	0.378	0.47
40	2.95	2.41	27.36	16.85	0.384	0.36
50	3.03	2.39	27.61	16.87	0.389	0.34
60	3.00	2.40	27.87	17.08	0.387	0.32
70	2.99	2.40	27.91	17.11	0.387	0.36
80	2.30	2.62	28.95	19.13	0.339	0.33
90	2.29	2.62	30.07	19.90	0.338	0.35

n with PbF_2 content. The first is for $PbF_2 \leq 50$ mol%. In this region, n decreases with increasing the content of PbF_2. The second is for $50 \leq PbF_2 \leq 70$ mol% where n is constant. The last one is that for $PbF_2 > 70$ mol% where n increases with increasing PbF_2 content. The n value varies from 2.39 to 2.62. These variations are due to the same structural changes that affect the variation of E_g. Further, because energy gap is inversely proportional to refractive index according to Eq. (9), the structural changes and the variation of both $C_{Pb(f)}$ and $C_{Pb(m)}$ with PbF_2 [8] are responsible for the change of n. It is assumed that in the first region, the increase and decrease of $C_{Pb(f)}$ and $C_{Pb(m)}$, respectively, limit the NBO formation and hence n decreases.

3.3.2 Molar refractivity and metallization criterion

The molar refraction (R_m) of the studied glasses and glass–ceramics was estimated using the Lorentz-Lorentz equation,

$$R_m = \left(\frac{n^2 - 1}{n^2 + 2}\right) V_m \tag{10}$$

Figure 9 shows that the molar refraction is nearly constant for $PbF_2 \leq 70$ mol% and then increases from 17.11 to 19.9 cm^3 for further additions from PbF_2. This behavior is similar to that of the molar volume and the refractive index with PbF_2 content as shown in Figs. 1 and 8, respectively. This behavior is due to the dependence of the molar refraction on the refractive index and molar volume.

The following equation is used to estimate the metallization criterion (M) for PbF_2–TeO_2 glasses and glass–ceramics [29],

$$M = 1 - \frac{R_m}{V_m} \tag{11}$$

M anticipates the way of behaving of glass materials to metallization or insulation depending on the values of R_m and V_m [31]. Values of M change between 0.338 and 0.389 (Table 1), whereas Fig. 9 shows that M increases gradually for $PbF_2 \leq 70$ mol% and then decreases suddenly for further additions of PbF_2. This behavior is similar to that of E_g (Fig. 8). These trends reveal that the glass material is closer to metallization behavior than insulation for $PbF_2 \leq 70$ mol%. On contrary, for $PbF_2 > 70$ mol% the insulating behavior is the dominant one. These results are consistent with the electrical conductivity results as shown in Fig. 3 where $\log\sigma_{473}$ increases with increasing PbF_2 content for $PbF_2 \leq 50$ mol% then decreases steadily up to 90 mol% PbF_2.

3.3.3 Urbach energy

Urbach energy E_U characterizes the range of the exponential tail of the absorption edge. The relation between Urbach energy and the absorption tails is given by,

$$\alpha(\upsilon) = \alpha_o \exp\left(h\upsilon/E_U\right) \tag{12}$$

where E_U is the Urbach energy and α_o is a constant. Figure 10 shows plots for $\ln(\alpha)$ against photon energy, $E = h\upsilon$, for determination of the Urbach energy E_U. Figure 11 represents an example for estimating E_U [32].

Figure 12 shows the change of E_U with PbF_2 content. The values of E_U lie between 0.32 and 0.54 eV which are in the range of amorphous semiconductors [27, 33]. E_U decreases with increasing PbF_2 up to 50 mol% and seems to be constant for higher PbF_2 contents. This variation might be due to the formation of crystalline phases such as $Te_2O_3F_2$ and PbF_2 [8] which reinforces the possibility of formation of a matrix with a long-range order. This order in the glass

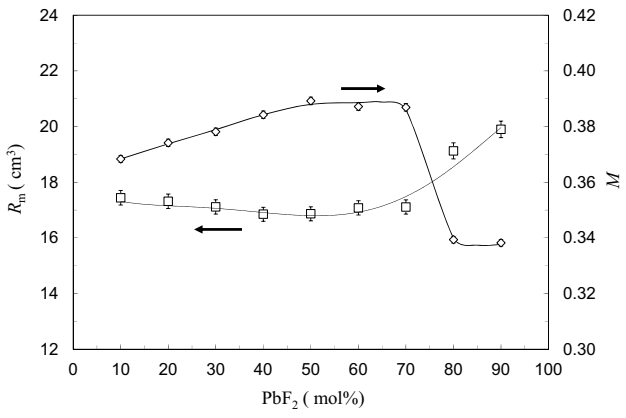

Fig. 9 Dependence of metallization criterion M and molar refractivity R_m on PbF_2 content

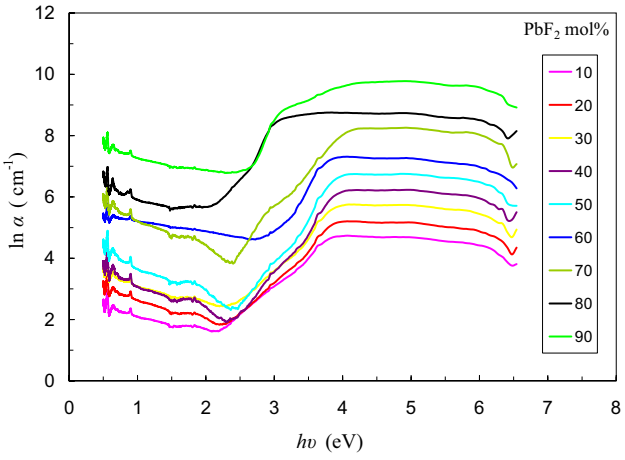

Fig. 10 Logarithm of the absorption coefficient, $\ln(\alpha)$, against photon energy, $h\upsilon$

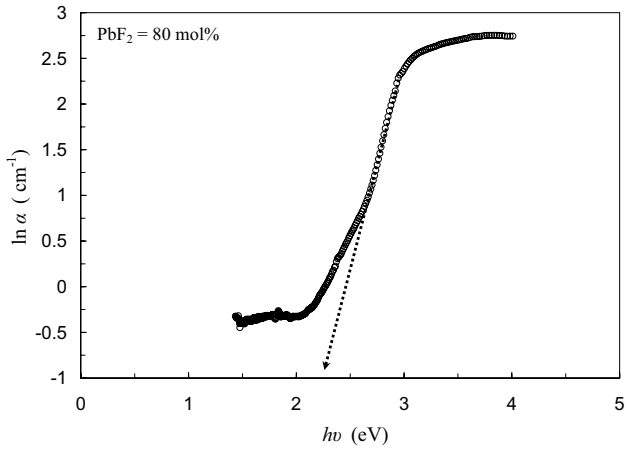

Fig. 11 Logarithm of the absorption coefficient, ln(α), against photon energy, $h\upsilon$ for the sample (PbF_2 = 80 mol%)

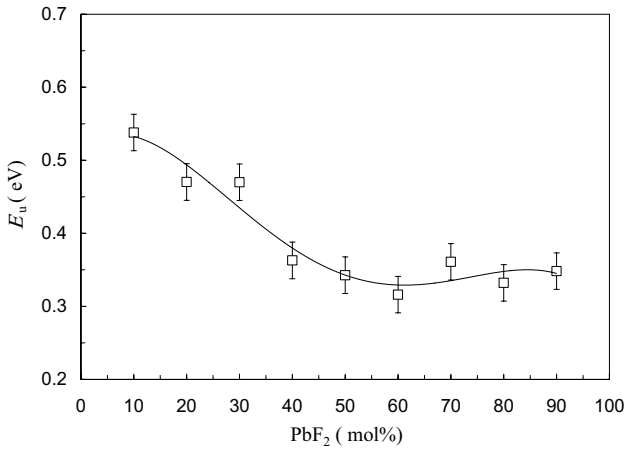

Fig. 12 Variation of the Urbach energy E_U with PbF_2 content in

contributes to a reduction of E_U. Analogous behavior of E_U was noticed with TiO_2 [27].

4 Conclusion

In PbF_2–TeO_2 glasses and glass–ceramics, D increases due to that the molecular mass of PbF_2 is larger than that of TeO_2. The change in V_f and P_d is responsible for the change in V_m. It is considered that Pb^{2+} ions are the main charge carriers. For $PbF_2 \leq 50$, the constancy of V_f causes a limited increase in conductivity. Whereas, for $PbF_2 > 50$ mol% the conductivity decreases because PbF_2 tends to form its own crystalline and amorphous matrix in the form of clusters. E_g increases with increasing PbF_2 content for $PbF_2 \leq 50$ mol%, then it decreases sharply then becomes constant for $PbF_2 > 70$ mol%. n changes in an opposite manner to that of E_g. E_U decreases with increasing PbF_2 up to 50 mol%. Then for further additions of PbF_2, it is nearly constant. These trends might be related to the structural variations that take place with modifying the network by PbF_2.

References

1. E. Kashchieva, Y. Ivanova, Electron microscopic investigations of microheterogeneous structure in glasses from the GeO_2-PbO-PbF_2 oxide-halide system. J. Mater. Sci. Lett. **10**, 1356–1358 (1991)
2. W. Akshatha, Y. Raviprakash, S.D. Kamath, Dielectric properties and relaxation dynamics in PbF_2-TeO_2-B_2O_3-Eu_2O_3 glasses. Trans. Nonferrous Met. Soc. China **25**, 2637–2645 (2015)
3. J.M. Reau, M. Poulain, Ionic conductivity in fluorine-containing glasses. Mater. Chem. Phys. **23**, 189–209 (1989). https://doi.org/10.1016/0254-0584(89)90024-2
4. H. Nasu, T. Uchigaki, K. Kamiya, H. Kanbara, K. Kubodera, Non-resonant-type third-order nonlinearity of (PbO, Nb_2O_5)-TiO_2-TeO_2 glass measured by third-harmonic generation. Jpn. J. Appl. Phys. **31**, 3899–3900 (1992). https://doi.org/10.1143/jjap.31.3899
5. W. Vogel, H. Burger, G. Zerge, B. Muller, K. Forkel, G. Winterstein, A. Boxberger, H. Romhild, Halogenid-und sulfathaltige telluritglaser. Silikattechnelk **25**, 207 (1974)
6. G. El-Damrawi, Transport behavior of PbO-PbF_2-TeO_2 glasses. Phys. Status Solidi **177**, 385–392 (2000)
7. S. Xu, G. Wang, J. Zhang, S. Dai, L. Hu, Z. Jiang, Composition dependent upconversion of Er^{3+}-doped PbF_2-TeO_2 glasses. J. Non. Cryst. Solids **336**, 230–233 (2004)
8. E.F. El Agammy, H. Doweidar, K. El-Egili, R. Ramadan, Structure of PbF_2–TeO_2 glasses and glass-ceramics. J. Mater. Res. Technol. **9**, 4016–4024 (2020). https://doi.org/10.1016/j.jmrt.2020.02.028
9. H. Doweidar, G. El-Damrawi, M. Abdelghany, Structure-properties correlations in PbF_2-B_2O_3 glasses. Phys. Chem. Glass. J. Glass Sci. Technol. Part B **55**, 121–129 (2014)
10. K. Barbalace, Periodic table of elements. Environ. Chem. Com., 4–14 (2007)
11. M. Burgess, D. McClarnon, M. Affatigato, S. Feller, Packing as a probe of structure in alkaline earth glass systems. J. Non. Cryst. Solids **354**, 3491–3502 (2008)
12. C. Kittel, P. McEuen, P. McEuen, *Introduction to Solid State Physics* (Wiley, New York, 1996)
13. E.F. El Agammy, H. Doweidar, K. El-Egili, R. Ramadan, M. Jaremko, A.H. Emwas, Structure of NaF–TeO_2 glasses and glass-ceramics. Ceram. Int. **46**, 18551–18561 (2020). https://doi.org/10.1016/j.ceramint.2020.04.161
14. Y. Jia, J. Lin, W. Zhang, C. Li, J. Ren, L. Rong, Structure and infrared emission of Ho^{3+}/Yb^{3+} Codoped TeO_2-ZnO-ZnX_2 (X=F, Cl, Br) glasses. J. Chin. Ceram. Soc. **42**, 545–556 (2014)
15. H. Doweidar, G. El-Damrawi, M. Abdelghany, Structure and properties of CaF_2-B_2O_3 glasses. J. Mater. Sci. **47**, 4028–4035 (2012)
16. A. Osaka, Y. Miura, T. Tsugaru, Bonding state of fluorine in lead-tin oxyfluorophosphate glasses. J. Non. Cryst. Solids **125**, 87–92 (1990)
17. W.S. AbuShanab, E.B. Moustafa, A.H. Hammad, R.M. Ramadan, A.R. Wassel, Enhancement the structural, optical and nonlinear optical properties of cadmium phosphate glasses by nickel ions. J. Mater. Sci. Mater. Electron. **30**, 18058–18064 (2019)
18. E.A. Davis, Nf. Mott, Conduction in non-crystalline systems V. Conductivity, optical absorption and photoconductivity in amorphous semiconductors. Philos. Mag. **22**, 903–922 (1970)
19. E.F. El Agammy, A.M.A. Mostafa, M. Al-Zaibani, H.O. Tekin, R. Ramadan, A. Essawy, S.A.M. Issa, Tailoring the structuralism in xBaO·(30-x) Li_2O·70B_2O_3 glasses for highly efficient shields of Gamma radiation and neutrons attenuators. Phys. Scr. (2021)

20. M.M. Hivrekar, D.B. Sable, M.B. Solunke, K.M. Jadhav, Different property studies with network improvement of CdO doped alkali borate glass. J. Non. Cryst. Solids **491**, 14–23 (2018)
21. A.H. Hammad, A.M. Abdelghany, Optical and structural investigations of zinc phosphate glasses containing vanadium ions. J. Non. Cryst. Solids **433**, 14–19 (2016)
22. S.Y. Marzouk, R. Seoudi, D.A. Said, M.S. Mabrouk, Linear and non-linear optics and FTIR characteristics of borosilicate glasses doped with gadolinium ions. Opt. Mater. (Amst) **35**, 2077–2084 (2013)
23. M.R. Sahar, N. Noordin, Oxychloride glasses based on the TeO_2-ZnO-$ZnCl_2$ system. J. Non Cryst. Solids **184**, 137–140 (1995)
24. A.M.A. Mostafa, E.F. El Agammy, M. Al-Zaibani, R. Ramadan, S.A.M. Issa, H.O. Tekin, Characterization of synthesized xBaO-(40-x)Li_2O-60B_2O_3 glass system: a multi-dimensional research on optical and physical properties. J. Mater. Sci. Mater. Electron., 1–19 (2021)
25. A.M.A. Mostafa, H.M. Zakaly, S.A. Al-Ghamdi, S.A. Issa, M. Al-Zaibani, R.M. Ramadan, E.F. El Agammy, PbO–Sb_2O_3–B_2O_3–CuO glassy system: evaluation of optical, gamma and neutron shielding properties. Mater. Chem. Phys. **258**, 123937 (2021). https://doi.org/10.1016/J.MATCHEMPHYS.2020.123937
26. E.F. El Agammy, H. Doweidar, K. El-Egili, R.M. Ramadan, Physical and optical properties of NaF–TeO_2 glasses and glass–ceramics. Appl. Phys. A. **127**, 42 (2021). https://doi.org/10.1007/s00339-020-04153-6
27. W. Stambouli, H. Elhouichet, M. Ferid, Study of thermal, structural and optical properties of tellurite glass with different TiO_2 composition. J. Mol. Struct. **1028**, 39–43 (2012)
28. M.S. Malik, C.A. Hogarth, The effect of chloride ions on the optical properties of TeO_2-CuO-$CuCl_2$ glasses. J. Mater. Sci. **25**, 116–120 (1990)
29. V. Dimitrov, S. Sakka, Electronic oxide polarizability and optical basicity of simple oxides. Int. J. Appl. Phys. **79**, 1736–1740 (1996)
30. J.A. Duffy, Chemical bonding in the oxides of the elements: a new appraisal. J. Solid State Chem. **62**, 145–157 (1986)
31. S.L.S. Rao, G. Ramadevudu, M. Shareefuddin, A. Hameed, M.N. Chary, M.L. Rao, Optical properties of alkaline earth borate glasses. Int. J. Eng. Sci. Technol. **4**, 25–35 (2012)
32. L. Skuja, K. Kajihara, Y. Ikuta, M. Hirano, H. Hosono, Urbach absorption edge of silica: reduction of glassy disorder by fluorine doping. J. Non. Cryst. Solids **345**, 328–331 (2004)
33. E.A. Davis, N.F. Mott, *Electronic Processes in Non-Crystalline Materials* (Clarendon Press, Oxford, 1971)